Experimental Uncertainty Analysis for Nondestructive Testing of the CSX Wilbur Bridge Using Electronic Distance Measurements to Measure 3-D Coordinates of Cardinal Points

David H. Parker

Parker Intellectual Property Enterprises, LLC, 3919 Deepwoods Road,

Earlysville, VA 22936, USA

david@parker-ip-ent.com www.parker-ip-ent.com (434) 975-3345

ABSTRACT

A 154 page report by Moreu and LaFave in 2012 explains unique problems railroad bridge engineers must contend with. The gross weight of cars went from 200,000 pounds to 263,000 pounds in the 1970s, and to 286,000 pounds in 1991. The ratio of live to dead loads are much greater for railroads than highways. Dynamic forces due to such things as wheel hunting, rock and roll, locomotive tractive forces, and braking make it very desirable to measure motions in all three directions, i.e., longitudinal, transverse, and vertical directions—which is why a survey of railroad bridge engineers ranked measuring 3-D deflections under live loads as the top research interest. It will be argued that electronic distance measurement instruments are uniquely qualified to perform such measurements. This is a technology that is unfamiliar to the bridge industry, so a feasibility study is needed. The CSX Railroad Wilbur Bridge (http://bridgehunter.com/ny/ulster/wilbur-railroad/) is a 270-foot span Parker through truss bridge, built in 1903, which is still in revenue service, and representative of US railroad bridges. The age, design, size, and geography make it a good selection for the feasibility study. Plans are presented for nondestructive testing and structural health monitoring of the structure by electronic distance measurement instruments in a trilateration/multilateration architecture. Instrument bench mark locations and cardinal points on the structure are identified. Uncertainty analyses are conducted for least squares adjustments using the Preanalysis feature of MicroSurvey® STAR*NET software, which calculates the uncertainty of a prescribed measurement plan, based on entered instrument performance specifications. The study was conducted for various combinations of measured distances in trilateration/multilateration architectures for distance measurements between 84 and 383 meters. Results are presented for both laser tracker and total station class electronic distance measurement instruments. Uncertainties are calculated for measured 3-D coordinates in the absolute reference coordinate system (which are directly dependent on the group refractive index of air), for differential measurements between adjacent cardinal points on the bridge (which are less dependent on the group refractive index), and for differential dynamic and vibrational measurements of individual points (which are insensitive to the group refractive index). Results confirm that the resultant 3-D coordinate uncertainties make the measurement architecture attractive to railway bridge engineers for conducting static and dynamic load testing, and structural health monitoring.

INTRODUCTION

This is the fourth in a series of papers on the use of electronic distance measurement (EDM) instruments for nondestructive testing (NDT) and structural health monitoring (SHM). The four papers are cumulative with each covering a different aspect of a common theme, so those interested in the subject should also review the first three papers (First Paper,[1] Second Paper,[2] Third Paper[3]) and a related family of US Patents.[4-7]

It is the thesis of this series of papers that the use of EDM for NDT and SHM has largely been overlooked, or misapplied, outside of the aerospace, precision manufacturing, and shipbuilding industries. The technology transfer from these high technology industries presents significant opportunities in the civil, structural, mechanical, and software engineering fields, as well as expanded markets for instrument manufacturers, software companies, and service providers—particularly for large-scale static and dynamic metrology applications, such as bridges. The Third Paper[3] argues that there is a major disconnect between the bridge engineering, NDT, and the Coordinate Metrology Society Conference (CMSC) communities—which this paper is intended to address with the CMSC community by example of a railroad bridge application.

MEASUREMENTS DESIRED BY RAILROAD BRIDGE ENGINEERS

Railroad bridge engineers must contend with even greater challenges than highway bridge engineers due to the high ratio of live to dead load, large dynamic forces, and increasing heavy axle loads (HAL) due to increasing gross vehicle weight (GVW), which has gone from 200,000 pounds in the 1970s to 286,000 pounds in 1991.[8] Dynamic forces are due to such things as wheel hunting, wheel flat spots, high center of gravity loads which induce rock and roll, locomotive tractive forces, braking forces, and discontinuities in stiffness at approaches.[9-13]

Moreu and LaFave published an extensive 154 page report[14] in 2012 (The 2012 Report) in which they interviewed sixteen experts on railway bridges and structural engineering, with a combined experience of more than 500 years, as to research priorities for railway bridges.

There are a number of findings in The 2012 Report that are particularly relevant to the CMSC community, which are worth mentioning in arguments establishing the need for high accuracy 3-D measurements, and Level-Two Laser Tracker Metrologist to conduct NDT measurements.

The present state-of-the-art for SHM of bridges is to instrument the bridge with accelerometers, inclinometers, strain gages, extensometers, and temperature sensors. The 2012 Report addresses the problems of using accelerometers, which must be integrated twice, to measure displacement. Item 8 states (p. 82):

> Finally, railroad bridge structural engineers showed specific interest in developing sensors that could collect the actual displacement of railroad bridges in real-time. In their opinion, displacement data could be of significant assistance for railroad bridge managers. However, these structural engineers expressed their concern of sensors being able to integrate acceleration records due to the Rigid Body Motion (RBM) intrinsic effect to the sensor

being accelerated. This group of railroad bridge structural engineering experts showed interest in developing sensing tools and methods that can accurately measure real-time displacements of bridges under train traffic, in the three directions (longitudinal, transverse, and vertical).

Section 8.1 of The 2012 Report, states (p. 123):

This survey-based study ranked measuring deflections under live loads as the current top research interest. According to the majority of the engineers in the survey, measuring real-time deflections under live load can be beneficial both in terms of railroad bridge management and railroad bridge replacement prioritization, especially for timber bridges.

It will be argued that the proposed EDM measurements will provide hard, static and dynamic, dead and live load, high accuracy, measurement data; from the field, for a large number of cardinal points on actual bridges, under actual operating load conditions, in the vertical, longitudinal, and transverse directions; that are repeatable, traceable to NIST, intuitively understood, and economical; which will assist in a global structural assessment of the bridge. In other words, more than the engineers in The 2012 Report wished for.

AN OVERVIEW OF EDM CAPABILITIES

The First Paper[1] includes a section on AN INTRODUCTION TO ELECTRONIC DISTANCE MEASUREMENT, which will not be duplicated here. For the immediate purposes of this paper, attention will be drawn to the capabilities and possible applications. The First Paper also includes an extensive review of the literature on previous attempts to measure bridges using EDM--and explains why those attempts were misapplications of the instruments used.

The Second Paper[2] (which was presented at CMSC 2017) covers a review of commercially available EDM instruments and arguments as to why the radial measurement capabilities are understated in the instrument companies published specifications.

Commercially available laser tracker instruments measure extremely accurately in the radial direction, but much less accurately in the two angles. However, full three dimensional capabilities are available by using three instruments in a trilateration architecture, i.e., measuring the distances by EDM from three instruments attached to stable ground monuments. This is explained in detail in US Patent application publication 2016/0274001.[7] One can think of the architecture as a network of virtual extensometers, or strain gages, with one end attached to an accurately surveyed point on the ground, and the other end attached, with a clear line of sight, to a cardinal point on a bridge.

TABLE 1 is a summary of published laser tracker instrument specifications showing the accuracies for range only. The much less accurate angles are generally about the same as a theodolite, i.e., about one arc second, or approximately 5 parts-per-million (5 μm/m), in each axis.

High end total stations, intended for general surveying and construction, are much less accurate in range measurements than laser trackers and the measurements are much slower.

However, the published range specifications are much longer, and the accuracies have improved to the point that they may be adequate for some quasi static SHM applications. For comparison purposes, a summary of published specifications for representative high end total stations is shown in TABLE 2. This paper is directed to high accuracy, so unless specifically stated otherwise, EDM instruments will be assumed to be laser tracker class instruments in the discussion.

Note that the published specification ranges of the currently available commercial laser tracker instruments are, it has been argued,[2] artificially limited to relatively short distances, i.e., 80-160 m. The specification ranges are more than sufficient for present customer instrument applications, but need to be longer for most bridge applications. The artificial range limitation is due to the inherent limitations of angle measurements and the need to specify the maximum permissible error (MPE) of 3D coordinates, as per the ASME B89.4.19 standard[15] traditionally used in the industry, and the fact that heretofore there has been little market demand for longer range specifications. This is not a limitation of the accuracy of EDM, which the table shows has been used at 4,000 meters by the Kern ME5000 Mekometer, and 1,000 meters for the NRAO PSH97. The need for instrument manufacturers to provide full specifications of instrument capabilities is a subject addressed in detail in the Second Paper.[2]

Unfortunately, the literature is limited on published experimental data that properly uses EDM for SHM applications. The discontinued ME5000 Mekometer is manually pointed and has no angle measurement transducers. The National Radio Astronomy Observatory (NRAO) Green Bank Telescope (GBT) is a 100 meter radio telescope built in the 1990s. At that time, the best commercially available instruments were total stations with a radial accuracy of around 3 mm. As part of the GBT project, NRAO built 20 custom EDM instruments, which they called the model PSH97, as shown in TABLE 1. Example measurement results are in the earlier papers[1-3] and will not be reproduced here.

As explained in more detail in the Third Paper,[3] modern EDM instruments are far superior to the early PSH97 instruments in every respect—except on paper.

Based on the published specifications alone, an engineer would probably not attempt to make the measurements proposed in this paper with any of the modern instruments, due to the apparent distance and measurement speed constraints. Yet, the PSH97 experimental data demonstrated the proof of principle over 20 years ago.

AN EXAMPLE BRIDGE MEASUREMENT ARCHITECTURE

An example will illustrate the measurement architecture and utility. FIGURE 1 shows a plan view of the CSX Wilbur Bridge over Rondout Creek in Kingston, NY. According to Bridgehunter.com,[16] the 1,232 foot long railroad bridge, built in 1903, includes a 269.7 foot long, Parker through truss bridge over the creek. Based on the US Geological Survey (USGS) Quadrangle Topo maps for Kingston East, and Kingston West, NY, the rail is at an elevation of about 150 feet, and the creek is at an elevation of about 10 feet.

As explained in the First Paper,[1] in order to fully exploit the high accuracy of EDM, it is necessary to measure by trilateration, i.e., three distances must be measured from accurately measured locations in the coordinate frame of reference, such as stable concrete ground monuments, or bench marks. Ideally, the three distances are from orthogonal directions for the strongest 3-D measurements. In practice, it is seldom that three orthogonal measurements can be made, so it is important to optimize instrument and target locations in order to optimize the measurements for the desired parameters being measured. For added accuracy, more than three measurements are made in a multilateration architecture and a least squares adjustment of the measurements is made.

For example, if the only interest is vertical deflections, a single instrument located under the bridge may be sufficient. However, for SHM applications, the objective is to detect anomalies that are unpredictable, i.e., in general, there are almost an infinite number of failure possibilities. The more unusual the deviation is from nominal, the more interesting the measurements are.

A good example is a fracture of the top cord of the Delaware River Bridge in 2017.[17] Measurements of the 3-D coordinates of a number of cardinal points on the bridge would have indicated an anomaly that would have prompted a closer visual inspection. Quite likely, changes in the coordinates and dynamic performance characteristics would have been significant enough to have raised awareness before the crack progressed to a full fracture. This is one reason why, in general, full 3-D coordinate measurements are desirable.

As explained in the section above, railroad bridge engineers are not only interested in the vertical deflections, but also particularly interested in the transverse and longitudinal motions of railroad bridges—for both static and dynamic motions.

FIGURE 1 shows a Google Earth plan view of the bridge with bench mark locations BM101-BM107 indicated, which have been chosen for evaluation as one of the best practical EDM instrument locations for measurements of cardinal points on the bridge, with an emphasis on measuring the transverse, longitudinal, and vertical motions.

The coordinates, in NAD83, for BM101-BM107 and the center of the through truss span were estimated from the USGS maps. The height of the bridge, above the rail, was estimated from the photograph[18] in FIGURE 2 to be around 50 feet. TABLE 3 lists the coordinates of BM101-BM107 and the top and bottom of the center of the through truss span. It also includes the approximate slope distances between the bench marks and the top and bottom of the center of the bridge, which vary between around 84 to 383 meters.

Note that BM101 is at approximately the same elevation as the bridge, and lines of sight to the northeast side of the bridge are somewhat perpendicular to the track, which makes distance measurements for transverse movements, along the lines of sight, very accurate; but insensitive to vertical and longitudinal movements.

BM102 and BM103 are near the creek level, with lines of sight looking up to the northeast side of the bridge. These measurements are very sensitive to vertical deflections,

transverse movements, and longitudinal movements. By combining all three distance measurements, a high accuracy 3-D coordinate may be determined.

BM104 is high on a mountain with lines of sight overlooking the southwest side of the bridge. The geometry makes the measurements sensitive to transverse, and longitudinal movements, but less sensitive to vertical movements. BM105 is near the creek level with lines of sight looking up to the underside of the bridge. The geometry makes the measurements sensitive to longitudinal and vertical movements, but less sensitive to transverse movements. BM106 is high on a mountain with lines of sight perpendicular to the track. Like BM101, measurements are sensitive to transverse movement, but less sensitive to vertical and longitudinal movements.

BM107 is above the tunnel and above the top of the bridge with lines of sight down the track. The geometry makes the measurements sensitive to longitudinal movement, but insensitive to transverse and vertical movements. For measurements of the top of the bridge, BM107 can be combined with BM101-BM103 on the northeast side, and BM104-BM106 on the southwest side.

FIGURE 2 shows a photo[18] of the southwest side of the bridge from a location on the ground west of BM105, which is offset from the northwest tower, under BSW119. Bridge cardinal points of the joints on the southwest side are identified as BSW101-BSW119, with corresponding cardinal points BNE101-BNE119 symmetrically located on the northeast side.

Passive retroreflector targets are permanently attached to the cardinal points with references which provide for replacement over the years, such as stainless steel weld plates with dowel pin connections for the retroreflectors. Conventional survey retroreflectors have a limited angle of acceptance. In order to provide for wide angles of acceptance, special retroreflector assemblies are required[19,20] which virtually reflect from a common point—thus eliminating any Abbe errors.

FIGURE 3 shows a Google Earth view of cardinal points on the southwest side from near BM106, and FIGURE 4 shows a Google Earth view of cardinal points on the northeast side of the bridge from behind BM101.

In a typical NDT scheme, the bench marks would be permanently established by concrete columns with provisions to accurately position EDM instruments over the bench marks. The bench marks would be accurately surveyed to establish a fixed coordinate system that would exceed the life of the bridge. Auxiliary bench marks may be desired in order to reference the instrument to them. In other words, by measuring the distances to three, or more, reference bench marks, the instrument location is determined.

With the retroreflector targets already permanently in place, a survey crew, working under the direction of a Level-Two Certified Laser Tracker Metrologist (certified by the Coordinate Metrology Society), would mount and operate the portable EDM instruments.

A series of measurements would be conducted, via remote control, from a central control location, for various load conditions. The measurements would be adjusted, in near real-time, to determine the 3-D coordinates of all cardinal points. After the data is reviewed, the survey crew would remove the instruments and proceed to the next bridge to be tested.

UNCERTAINTY ANALYSIS

In preparation for a measurement campaign, it is always recommended to conduct an uncertainty analysis[21] while in the planning stages. This will ensure an optimum selection of instruments, target locations, and measurement locations. EDM instrument manufacturers' customers tend to be highly sophisticated metrologists working in high technology industries and government laboratories--which would quickly detect and call them out for not actually meeting published specifications. Therefore, the published specifications tend to err on the side of being overly conservative, and the actual measurements are conducted by automated instruments. The net result is that measurement uncertainties are highly predictable with a bias toward the conservative side.

An uncertainty analysis was run for various measurements under various assumptions for instrument specifications using the Preanalysis feature of the Star*Net 9 software package, by MicroSurvey ® Inc.

Star*Net allows one to virtually conduct a survey, based on a measurement plan and assumptions of instrument locations, target locations, and instrument uncertainty parameters. Assumptions are weighted by selected values and a least squares adjustment is made using the virtual measurements. A sample Star*Net output listing is included in Appendix A.

Most EDM instrument specifications are for MPE, instead of the standard deviation. In such cases, NIST Technical Note 1297, section 4.6 [21] recommends dividing by $\sqrt{3}$ to obtain the standard uncertainty. For the purpose of this paper, the more conservative assumption will be made to use the MPE as the standard deviation. The results are summarized in TABLE 4.

In this Preanalysis software run, the coordinates of the instrument locations BM101-BM107 were assumed to be absolute and held fixed in the adjustments. While Star*Net can handle thousands of points, this paper will only use two points as an example. The top and bottom of the center of the span were used as approximate coordinates for a representative pair of cardinal points on the span. For the Preanalysis, the top node was given names BNE_T and BSW_T using the same coordinates for the center top in TABLE 3; and the bottom node was given names BNE_B and BSW_B using the same coordinates for the center bottom in TABLE 3. By assigning two names to each node, Star*Net treats them as independent nodes, which allows for possible differences in visibility. For example, some instruments may have clear lines of sight to nodes on the northeast side, but not the southwest side, while others may have clear lines of sight to both.

Referring to TABLE 4, the first group of simulations assume the EDM instruments point with an accuracy of 5 seconds and measure range with an accuracy of 10 μm + 1 part-per-million (ppm). For example, the error in distance for a measurement at 100 meters would be 110 μm, and at 200 meters would be 210 μm, etc. The pointing accuracy of 5 seconds would be around 25 ppm, or 2,500 μm at 100 m and 5,000 μm at 200 m. For all practical purposes, the 5 second accuracy makes the angles irrelevant in the trilateration adjustment. Changing it to 50 seconds would not significantly alter the results of the adjustment.

The first case is for measuring from BM101, BM102, and BM103 to the northeast side of the top of the center of the span in a set of trilateration measurements, i.e., BNE_T. Note, as a point of reference, that 100 μm is the thickness of a sheet of standard printer paper.

The adjustment shows that one could expect the standard deviation of the coordinates calculated by those measurements, under the assumptions made, in the N, E and elevation directions would be (428, 391, 1219) μm. The next assumption is that BNE_T was measured from all instrument locations BM101-BM107 in a set of multilateration measurements. Note that the standard deviations of (215, 121, 268) are a significant improvement over simply measuring from BM101-BM103--particularly in elevation.

In contrast, measurements from BM104, BM105, and BM106 to the south west side of the top of the center of the span in a set of trilateration measurements, i.e., BSW_T, is much stronger in elevation (336, 351, 447). This is primarily due to the strategic location of BM105 almost under the bridge, which is very sensitive to vertical movement of the bridge. Other combinations of measurements are included in TABLE 4.

For absolute accuracy of the coordinates of cardinal points, traceable to NIST, these standard deviations are about what one could expect. However, for a better understanding, one must analyze the sources of the errors. The assumption of a fixed 10 μm instrument error is probably not of much concern. The 1 ppm error warrants more consideration.

It is well known that EDM measurements are dependent on the speed of light, which is dependent on the group refractive index (GRI) of the air. The GRI of air is most dependent on temperature (about 1 part-per-million/C^o), and to a lesser amount on humidity, and pressure. Recall that the thermal coefficient of expansion for steel is around 11 ppm/C^o, which must be taken into consideration when analyzing the bridge performance.

The easiest way to correct for the group refractive index, in the outdoors, is to use reference distances as refractometers[22]. For example, if measurements are made from the instruments to fixed points, through a representative environment, the apparent distances will change due to changes in the GRI and the ratio of the distances. In other words, the GRI can be modeled out of the errors.

It should be noted that care must be taken to ensure a uniform environment. As with all high accuracy surveys, measurements should be made at night or under uniform cloud cover, for best results.

Uncertainty in the GRI is the source of the typical 1 ppm error used for laser trackers. It is noteworthy that this is a systematic error--not a random error. If one is actually concerned with differential movements, such as the movements between two joints, or how the bridge moves under loading, such as those measurements shown in the earlier papers for vibrations,[1-3] the uncertainties of differential motions are much less than 1 ppm.

The lower part of TABLE 4 is for the same cases, except assuming a 0.1 ppm instrument uncertainty--which experience has shown is a more realistic assumption for differential movement between adjacent points. Note the dramatic reduction in the standard deviations. For

example, for BNE_T measured by BM101-BM103, the uncertainties go from (428,391,1219) to (58, 55, 172); and for BNE_T from BM101-BM107 from (215, 121, 268) to (29, 17, 41). Deflections due to a high-rail vehicle crossing the bridge would be measurable.

TABLE 5 shows similar simulations for total stations with 600 μm and 800 μm errors. As with laser trackers, the 1 ppm error is systematic. However, the 600 μm and 800 μm fixed errors are not systematic, so they tend to dominate the adjustments. Depending on the objective, this may be acceptable for a particular study.

ANALYSIS OF MEASUREMENTS IN LIGHT OF BRIDGE ENGINEERS DESIRES

Turning now to how such high accuracy measurements may be used in a global structural assessment of the bridge. From TABLE 4, the smallest standard deviations are for the case where BNE_T is measured by all instruments BM101-BM107; (215, 121, 268) for 1 ppm and (29, 17, 41) for 0.1 ppm. Due to visibility constraints, this is probably not a realistic case. A more practical architecture is measuring BSW_T from BM104-BM107 and measuring BSW_B from BM104-BM106. Note that BM107, above the tunnel, has clear lines of sight to the top of the bridge, but not the bottom of the bridge. For the 1 ppm case, the standard deviations are (308, 296, 329) and (353, 326,581). For the 0.1 ppm case, the standard deviations are (40, 38, 48) and (47, 42, 83).

Referring to FIGURE 2, these accuracies would be indicative of the standard deviations for cardinal points BSW108 and BSW109. The combined standard deviation for differential measurement of the length of the member connecting the two joints would typically be estimated by taking the root sum square (RSS) of the elevation components of 48 and 83 μm, which would be 96 μm. Assume the length between BSW108 and BSW109 is 15 m, the standard deviation in a strain measurement would be 6.4 micro strain.

It can be argued that the standard deviation in the length between any pair of joints would be comparable. This would include between the BSW and BNE sides, and the diagonals e.g., between BSW108 and BNE108; and between BSW108 and BNE110. The strain in the members connecting the 36 joints could be determined from the coordinate measurements, i.e., it would virtually be like having wireless strain gages installed on the 104 members of the structure.

One interesting experiment would be to measure the coordinates of the 36 cardinal points under no live load conditions and then with a locomotive parked in the center of the span. In addition to the vertical deflections, it would be interesting to measure the transverse and longitudinal motions. Asymmetries in motions would be particularly interesting. Hysteresis would also be interesting when the live load is removed.

Another interesting experiment would be to measure motions while a locomotive is pulling cars across the bridge, i.e., introducing longitudinal forces on the structure. For example, slowly move onto the bridge and stop with the locomotive in the middle of the span. Then, apply predetermined longitudinal forces to start the train moving. This would also need to be measured for the locomotive pushing the cars and the locomotive approaching from opposite ends of the bridge in order to see if the abutments are symmetric.

Yet another interesting experiment would be to measure the cardinal points under braking conditions—in both directions. One would expect the motions due to the distributed longitudinal forces exerted by rail cars to be different from the localized longitudinal force exerted by a locomotive.

Still another interesting experiment would be to measure the cardinal points for trains passing at various speeds to subject the bridge to wheel flat spots, wheel hunting, and rock and roll.[10]

CONCLUSION

It has been shown that proposed measurements of the CSX Wilbur Bridge by EDM meet all of the desired results of railroad bridge engineers in The 2012 Report—and then some. Specifically: the measurements are quantified and repeatable; performed on the actual bridge in question; performed under static and dynamic conditions; performed under experimental and revenue conditions; performed under dead and live loads; produce results in the vertical, longitudinal, and transverse directions; intuitively understood; measure strain; and economical. More than they wished for!

TABLE 1. Range and accuracy for laser trackers

Manufacturer	Model	Range	Accuracy	Data Rate
API Automated Precision	Radian	80 m	10 μm or 0.7 μm/m	?
FARO	Vantage	80 m	16 μm + 0.8 μm/m	1,000 points/sec
Kern (no longer available)	ME5000 Mekometer	4,000 m	200 μm + 0.2 μm/m	?
Leica	AT403	160 m	10 μm	?
Leica	AT960-LR	160 m	0.5 μm/m	1,000 points/sec
Nikon	MV351 HS	50 m	10 μm + 2.5 μm/m	2 sec/point
NRAO (no longer available)	PSH97	1,000 m	50 μm + 1 μm/m	1,000 points/sec

TABLE 2. Range and accuracy for representative total stations

Manufacturer	Model	Range	Accuracy	Data Rate
Leica	TS60	3,500 m	600 μm + 1 μm/m	2.4 sec/point
Topcon	MS05AX	3,500 m	800 μm + 1 μm/m	?
Trimble	S9HP	7,000 m	800 μm + 1 μm/m	?

TABLE 3. Estimated coordinates of instruments and center of bridge top and bridge bottom, with approximate slant distances to center of bridge top and bridge bottom.

Identifier	Lat N	Long W	Z ft/m	Center top m	Center bottom m
BM101	41-54-47.5	73-59-45.9	150/45.720	383	383
BM102	41-54-42.4	73-59-53.1	15/4.572	165	160
BM103	41-54-39.2	73-59-48.1	15/4.572	230	227
BM104	41-54-28.4	73-59-57.1	240/73.152	321	322
BM105	41-54-40.3	74-00-00.3	15/4.572	92	84

BM106	41-54-40.3	74-00-12.9	220/67.056	351	351
BM107	41-54-45.3	74-00-07.9	240/73.152	307	307
center top	41-54-38.8	73-59-57.8	200/60.960		
center bottom	41-54-38.8	73-59-57.8	150/45.720		

TABLE 4. Standard deviation of measured points for laser trackers.

From	To	N μm	E μm	Z μm
10 μm + 1 ppm				
BM101-BM103	BNE_T	428	391	1219
BM101-BM107	BNE_T	215	121	268
BM104-BM106	BSW_T	336	351	447
BM104-BM107	BSW_T	308	296	329
BM101-BM103	BNE_B	397	355	1417
BM101-BM103, BM105	BNE_B	372	150	569
BM104-BM106	BSW_B	353	326	581
10 μm + 0.1 ppm				
BM101-BM103	BNE_T	58	55	172
BM101-BM107	BNE_T	29	17	41
BM104-BM106	BSW_T	44	45	63
BM104-BM107	BSW_T	40	38	48
BM101-BM103	BNE_B	55	51	206
BM101-BM103, BM105	BNE_B	54	22	86
BM104-BM106	BSW_B	47	42	83

TABLE 5. Standard deviation of measured points for total stations.

From	To	N μm	E μm	Z μm
600 μm + 1 ppm				
BM101-BM103	BNE_T	1192	1010	2377
BM104-BM106	BSW_T	821	814	1279
BM101-BM103	BNE_B	1161	936	2513
BM104-BM106	BSW_B	827	765	1408
600 μm + 0.1 ppm				
BM101-BM103	BNE_T	910	815	2046
BM104-BM106	BSW_T	606	590	1099
BM101-BM103	BNE_B	894	754	2228
BM104-BM106	BSW_B	621	561	1252
800 μm + 1 ppm				
BM101-BM103	BNE_T	1404	1164	2544
BM104-BM106	BSW_T	946	937	1464
BM101-BM103	BNE_B	1375	1091	2644
BM104-BM106	BSW_B	945	889	1550
800 μm + 0.1 ppm				
BM101-BM103	BNE_T	1155	997	2331
BM104-BM106	BSW_T	760	742	1335
BM101-BM103	BNE_B	1137	928	2473

BM104-BM106	BSW_B	769	709	1452

FIGURE 1. Google Earth plan view of CSX Wilbur Bridge showing instrument locations.

FIGURE 2. View of cardinal points on southwest side from near creek level. Photo taken by Joseph.[16, 18]

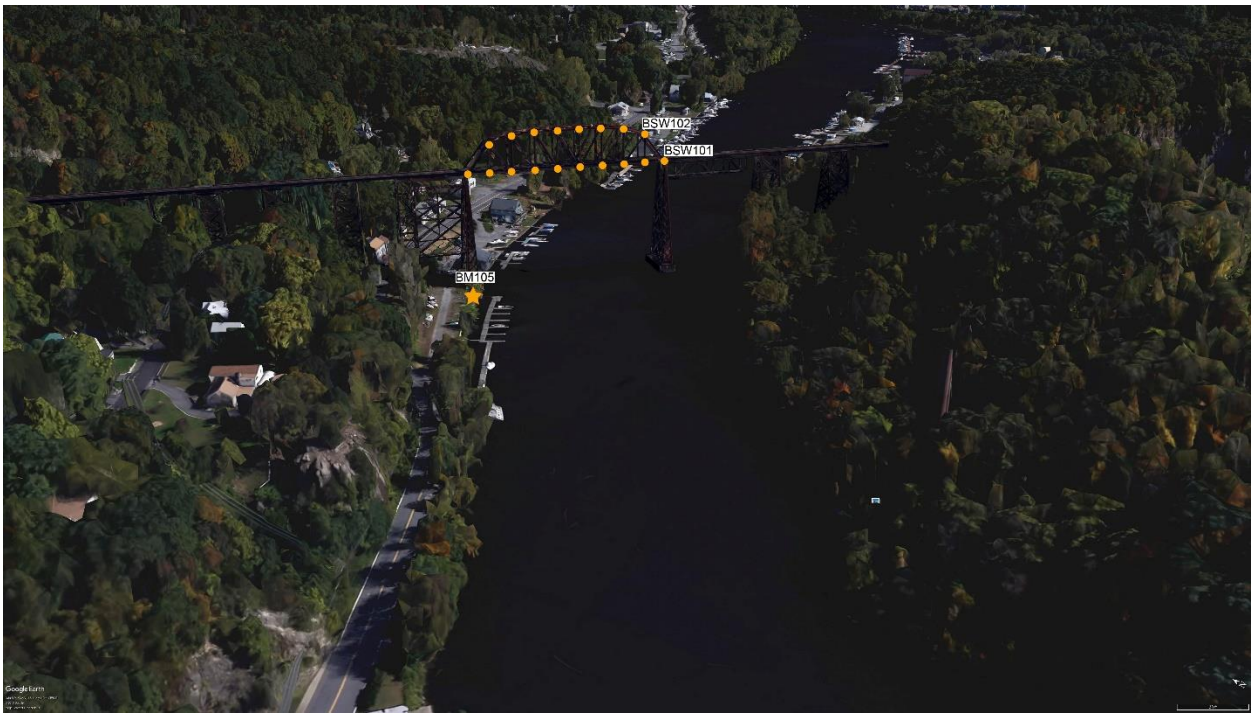

FIGURE 3. Google Earth view of cardinal points on southwest side from near BM106.

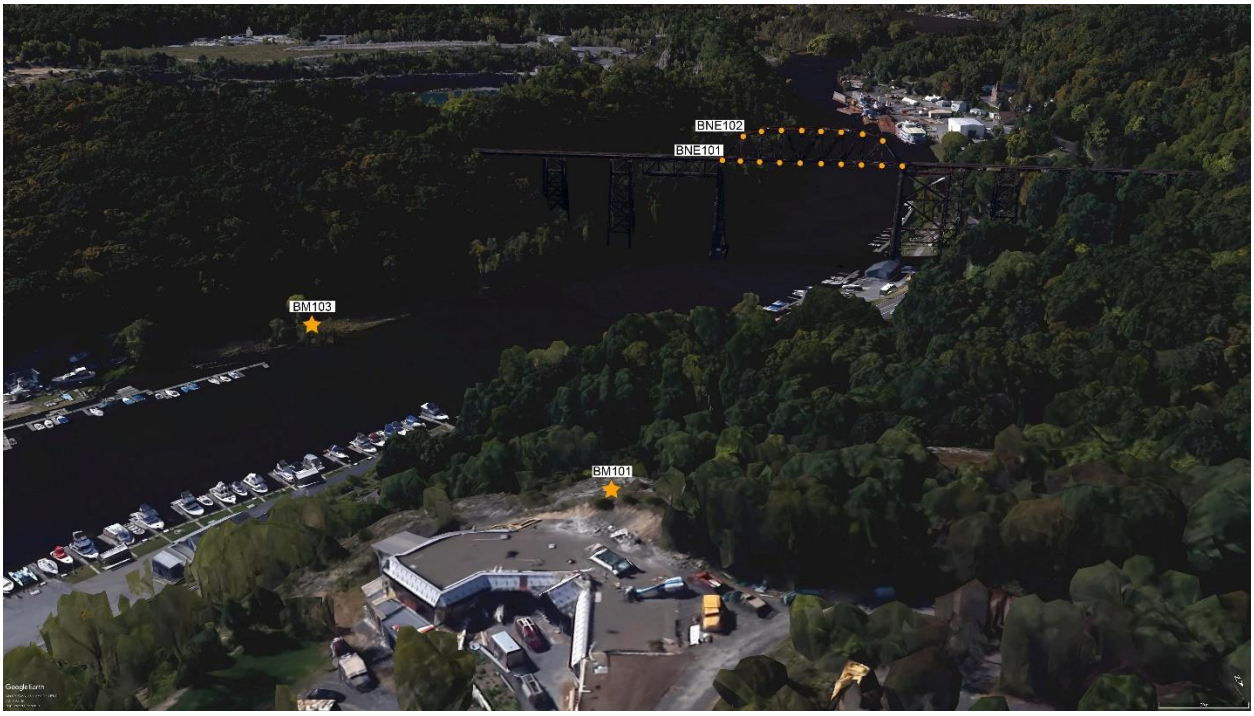

FIGURE 4. Google Earth view of cardinal points on northeast side from behind BM101.

REFERENCES

[1] Parker, D.H., Nondestructive testing and monitoring of stiff large-scale structures by measuring 3-D coordinates of cardinal points using electronic distance measurements in a trilateration architecture. In *Conference on Nondestructive characterization and monitoring of advanced materials, aerospace, and civil infrastructure 2017, Portland, OR*, volume 10169 of *Proceedings of SPIE*. SPIE, March 2017. paper 1016918.

[2] Parker, D.H., Using electronic distance measurement instruments in NDT and structural health-monitoring applications. *Quality Digest*, August 2017. Paper given at CMSC 2017, Snowbird, UT, original title "Opportunities for the use of electronic distance measurement instruments in nondestructive testing and structural health monitoring applications and how instrument manufacturers can facilitate early adopters in new fields".

[3] Parker, D.H., Opportunities for the use of electronic distance measurement instruments in nondestructive testing and structural health monitoring and implications for ASNT. In *Proceedings of 27th ASNT Research Symposium, Orlando, FL*. American Society for Nondestructive Testing, March 2018.

[4] Parker, D.H., and Payne, J.M., *Method for measuring the structural health of a civil structure*, 2011. US Patent 7,895,015.

[5] Parker, D.H., and Payne, J.M., *Methods for modeling the structural health of a civil structure based on electronic distance measurements*, 2012. US Patent 8,209,134.

[6] Parker, D.H., and Payne, J.M., *Methods for measuring and modeling the structural health of pressure vessels based on electronic distance measurements*, 2016. US Patent 9,354,043.

[7] Parker, D.H., and Payne, J.M., *Methods for measuring and modeling the process of prestressing concrete during tensioning/detensioning based on electronic distance measurements*, 2016. US Patent Application Publication 2016/0274001.

[8] Martland, C.D., Introduction of heavy axle loads by the north American rail industry. *Journal of the Transportation Research Forum*, 52(2):103–125, 2013.

[9] Moreu, F., LaFave, J.M., and Spencer, B.F., New regulations on railroad bridge safety: Opportunities and challenges for railroad bridge monitoring. In *Proceedings of SPIE, Sensors and Smart Structures Technologies for Civil, Mechanical, and Aerospace Systems 2012*, volume 8345, pages 834540–1 through 11, 2012.

[10] Moreu, F., Jo, H., Li, J., Kim, R.E., Cho, S., Kimmle, A., Scola, S., Le, H., Spencer, B.F. Jr., and LaFave, J.M., Dynamic assessment of timber railroad bridges using displacements. *Journal of Bridge Engineering*, page 04014114, 2014.

[11] Moreu, F., Li, J., Jo, H., Kim, R.E., Scola, S., Spencer, B.F. Jr., and LaFave, J.M., Reference-free displacements for condition assessment of timber railroad bridges. *Journal of Bridge Engineering*, page 04015052, 2015.

[12] Hoag, A., Hoult, N.A., Take, W.A., Moreu, F., Le, H., and Tolikonda, V., Measuring displacements of a railroad bridge using DIC and accelerometers. *Smart Structures and Systems*, 19(2):225–236, 2017.

[13] Moreu, F., Garg, P., and Ayorinde, E., Railroad bridge inspections for maintenance and replacement prioritization using unmanned aerial systems (UAS) with laser capabilities. In *TRB Annual Meeting*, number paper 18-06761. TRB, TRB, January 2018.

[14] Moreu, F., and LaFave, J.M., *Current Research Topics: Railroad Bridges and Structural Engineering, NSEL Report Series, Report No. NSEL-032*. Newmark Structural Engineering Laboratory, Department of Civil and Environmental Engineering, University of Illinois at Urbana-Champaign, October 2012.

[15] ASME. *ASME B89.4.19-2006 Performance Evaluation of Laser-Based Spherical Coordinate Measurement Systems*. The American Society of Mechanical Engineers, 2006.

[16] Hicks, F., Harden, L., Vance, C., Martin, I., King, D., and Finigan, C., CSX-Wilbur Bridge, Ulster County, NY. Online, Bridgehunter.com, April 2012. http://bridgehunter.com/ny/ulster/wilbur-railroad/.

[17] Foden, A., Gentz, C., Van Brunt, Z., and Rue, D., Structural monitoring of the Delaware River Turnpike Bridge emergency repairs. In *2017 ASNT Annual Conference October 30-November 2, 2017 Proceedings*, pages 68–76. American Society for Nondestructive Testing, ASNT, October 2017.

[18] Joseph. *Photo taken by Joseph*, June 2011. License: Creative Commons Attribution-NonCommercial-ShareAlike (CC BY-NC-SA), BH Photo #239216 https://www.flickr.com/photos/josepha/5907193656/.

[19] Parker, D.H., Multidirectional retroreflector assembly with a common virtual reflection point using four-mirror retroreflectors. *Precision Engineering*, 29:361–366, 2005.

[20] Parker, D.H., *Multidirectional retroreflectors*, 2010. US Patent RE41877.

[21] Taylor, B.N., and Kuyatt, C.E., Guidelines for evaluating and expressing the uncertainty of NIST measurement results. NIST Technical Note 1297, National Institute of Standards and Technology, 1994.

[22] Parker, D.H., Methods for correcting the group index of refraction at the ppm level for outdoor electronic distance measurement. In *Proceedings ASPE 2001 Annual Meeting*, pages 86–87. American Society for Precision Engineering, 2001. Full presentation is available from The National Radio Astronomy Observatory (NRAO) Library, GBT Archive L0680.

APPENDIX A

```
            MicroSurvey STAR*NET-PRO Version 9,0,3,6298
                    Licensed for Demo Use Only
                Run Date: Sun Mar 04 2018 15:30:51


             Summary of Files Used and Option Settings
             =========================================

                   Project Folder and Data Files

Project Name       CSX WILBUR BRIDGE
Project Folder C:\USERS\DAVID\DOCUMENTS\MICROSURVEY\STARNET\EXAMPLES
Data File List  1. CSX Wilbur Bridge.dat

                     Project Option Settings

STAR*NET Run Mode                   : Preanalysis
Type of Adjustment                  : 3D
Project Units                       : Meters; DMS
Coordinate System                   : UTM83-18
Geoid Height                        : 0.0000 (Default, Meters)
Longitude Sign Convention           : Positive West
Input/Output Coordinate Order       : North-East
Angle Data Station Order            : At-From-To
Distance/Vertical Data Type         : Slope/Zenith
Convergence Limit; Max Iterations   : 0.010000; 10
Default Coefficient of Refraction   : 0.070000
Create Coordinate File              : Yes
Create Geodetic Position File       : Yes
Create Ground Scale Coordinate File : Yes
Create Dump File                    : Yes

                 Instrument Standard Error Settings

Project Default Instrument
  Distances (Constant)              :    0.000010 Meters
  Distances (PPM)                   :    1.000000
  Angles                            :    5.000000 Seconds
  Directions                        :    5.000000 Seconds
  Azimuths & Bearings               :    5.000000 Seconds
  Zeniths                           :    5.000000 Seconds
  Elevation Differences (Constant)  :    0.015240 Meters
  Elevation Differences (PPM)       :    0.000000
  Differential Levels               :    0.002403 Meters / Km
  Centering Error Instrument        :    0.000000 Meters
  Centering Error Target            :    0.000000 Meters
  Centering Error Vertical          :    0.000000 Meters
```

Summary of Unadjusted Input Observations

Number of Entered Stations (Meters) = 11

Fixed Stations Description	Latitude	Longitude	Elev
BM101	41-54-47.500000	73-59-45.900000	45.7200
BM102	41-54-42.400000	73-59-53.100000	4.5720
BM103	41-54-39.200000	73-59-48.100000	4.5720
BM104	41-54-28.400000	73-59-57.100000	73.1520
BM105	41-54-40.300000	74-00-00.300000	4.5720
BM106	41-54-40.300000	74-00-12.900000	67.0560
BM107	41-54-45.300000	74-00-07.900000	73.1520

Free Stations Description	Latitude	Longitude	Elev
BNE_T	41-54-38.800000	73-59-57.800000	60.9600
BNE_B	41-54-38.800000	73-59-57.800000	45.7200
BSW_T	41-54-38.800000	73-59-57.800000	60.9600
BSW_B	41-54-38.800000	73-59-57.800000	45.7200

Number of Measured Distance Observations (Meters) = 18

From	To	Distance	StdErr	HI	HT	Comb Grid	Type
BM101	BNE_T	383.9279	0.0004	0.000	0.000	0.9996767	S
BM101	BNE_B	383.6253	0.0004	0.000	0.000	0.9996778	S
BM102	BNE_T	165.0266	0.0002	0.000	0.000	0.9996797	S
BM102	BNE_B	160.4597	0.0002	0.000	0.000	0.9996809	S
BM103	BNE_T	230.8119	0.0002	0.000	0.000	0.9996798	S
BM103	BNE_B	227.5690	0.0002	0.000	0.000	0.9996810	S
BM104	BSW_T	321.4086	0.0003	0.000	0.000	0.9996742	S
BM104	BSW_B	322.3467	0.0003	0.000	0.000	0.9996754	S
BM105	BSW_T	92.9382	0.0001	0.000	0.000	0.9996795	S
BM105	BSW_B	84.5640	0.0001	0.000	0.000	0.9996807	S
BM106	BSW_T	351.0028	0.0004	0.000	0.000	0.9996744	S
BM106	BSW_B	351.5978	0.0004	0.000	0.000	0.9996756	S
BM104	BNE_T	321.4086	0.0003	0.000	0.000	0.9996742	S
BM106	BNE_T	351.0028	0.0004	0.000	0.000	0.9996744	S
BM105	BNE_B	84.5640	0.0001	0.000	0.000	0.9996807	S
BM105	BNE_T	92.9382	0.0001	0.000	0.000	0.9996795	S
BM107	BNE_T	307.3868	0.0003	0.000	0.000	0.9996740	S
BM107	BSW_T	307.3868	0.0003	0.000	0.000	0.9996740	S

Number of Zenith Observations (DMS) = 18

From	To	Zenith	StdErr	HI	HT
BM101	BNE_T	87-43-30.18	5.00	0.000	0.000
BM101	BNE_B	90-00-00.00	5.00	0.000	0.000
BM102	BNE_T	70-01-12.37	5.00	0.000	0.000
BM102	BNE_B	75-08-28.24	5.00	0.000	0.000
BM103	BNE_T	75-51-33.70	5.00	0.000	0.000
BM103	BNE_B	79-34-57.86	5.00	0.000	0.000
BM104	BSW_T	92-10-26.12	5.00	0.000	0.000

BM104	BSW_B	94-52-54.58	5.00	0.000	0.000
BM105	BSW_T	52-38-48.79	5.00	0.000	0.000
BM105	BSW_B	60-52-59.85	5.00	0.000	0.000
BM106	BSW_T	90-59-42.46	5.00	0.000	0.000
BM106	BSW_B	93-28-44.45	5.00	0.000	0.000
BM104	BNE_T	92-10-26.12	5.00	0.000	0.000
BM106	BNE_T	90-59-42.46	5.00	0.000	0.000
BM105	BNE_B	60-52-59.85	5.00	0.000	0.000
BM105	BNE_T	52-38-48.79	5.00	0.000	0.000
BM107	BNE_T	92-16-23.31	5.00	0.000	0.000
BM107	BSW_T	92-16-23.31	5.00	0.000	0.000

Number of Grid Azimuth/Bearing Observations (DMS) = 18

From	To	Bearing	StdErr
BM101	BNE_T	S44-56-42.44W	5.00
BM101	BNE_B	S44-56-42.44W	5.00
BM102	BNE_T	S43-36-41.88W	5.00
BM102	BNE_B	S43-36-41.88W	5.00
BM103	BNE_T	S86-10-14.86W	5.00
BM103	BNE_B	S86-10-14.86W	5.00
BM104	BSW_T	N03-32-48.24W	5.00
BM104	BSW_B	N03-32-48.24W	5.00
BM105	BSW_T	S51-53-41.47E	5.00
BM105	BSW_B	S51-53-41.47E	5.00
BM106	BSW_T	S83-05-30.30E	5.00
BM106	BSW_B	S83-05-30.30E	5.00
BM104	BNE_T	N03-32-48.24W	5.00
BM106	BNE_T	S83-05-30.30E	5.00
BM105	BNE_B	S51-53-41.47E	5.00
BM105	BNE_T	S51-53-41.47E	5.00
BM107	BNE_T	S49-55-11.13E	5.00
BM107	BSW_T	S49-55-11.13E	5.00

Adjusted Bearings (DMS) and Horizontal Distances (Meters)

(Relative Confidence of Bearing is in Seconds)

From	To	Grid Bearing	Grid Dist	95% RelConfidence		
				Brg	Dist	PPM
BM101	BNE_B	S44-56-41.83W	383.5695	0.44	0.0006	1.4414
BM101	BNE_T	S44-56-47.79W	383.5954	0.24	0.0004	1.0507
BM102	BNE_B	S43-36-38.63W	155.0383	1.07	0.0006	3.6604
BM102	BNE_T	S43-36-54.17W	155.0639	0.59	0.0004	2.6344
BM103	BNE_B	S86-10-47.95W	223.7753	0.85	0.0003	1.5139
BM103	BNE_T	S86-10-39.93W	223.8021	0.49	0.0003	1.3107
BM104	BNE_T	N03-32-38.08W	321.2046	0.19	0.0005	1.6447
BM104	BSW_B	N03-34-10.85W	321.0794	0.52	0.0009	2.6686
BM104	BSW_T	N03-34-29.86W	321.1017	0.48	0.0007	2.2823
BM105	BNE_B	S51-56-15.69E	73.8855	1.75	0.0008	10.2299
BM105	BNE_T	S51-55-07.74E	73.8714	1.20	0.0004	5.7387
BM105	BSW_B	S51-46-18.35E	73.8468	2.52	0.0008	10.2187
BM105	BSW_T	S51-46-09.66E	73.8099	2.51	0.0005	7.2761
BM106	BNE_T	S83-05-47.76E	350.9605	0.31	0.0003	0.8805
BM106	BSW_B	S83-04-19.96E	350.8412	0.52	0.0008	2.2288
BM106	BSW_T	S83-04-29.68E	350.8080	0.47	0.0007	1.9414
BM107	BNE_T	S49-55-31.71E	307.1375	0.28	0.0004	1.4059
BM107	BSW_T	S49-53-21.02E	307.0826	0.60	0.0005	1.7426

Error Propagation

Station Coordinate Standard Deviations (Meters)

Station	N	E	Elev
BM101	0.000001	0.000001	0.000001
BM102	0.000001	0.000001	0.000001
BM103	0.000001	0.000001	0.000001
BM104	0.000001	0.000001	0.000001
BM105	0.000001	0.000001	0.000001
BM106	0.000001	0.000001	0.000001
BM107	0.000001	0.000001	0.000001
BNE_T	0.000215	0.000121	0.000268
BNE_B	0.000372	0.000150	0.000569
BSW_T	0.000308	0.000296	0.000329
BSW_B	0.000353	0.000326	0.000581

Station Coordinate Error Ellipses (Meters)
Confidence Region = 95%

Station	Semi-Major Axis	Semi-Minor Axis	Azimuth of Major Axis	Elev
BM101	0.000000	0.000000	0-00	0.000000
BM102	0.000000	0.000000	0-00	0.000000
BM103	0.000000	0.000000	0-00	0.000000
BM104	0.000000	0.000000	0-00	0.000000
BM105	0.000000	0.000000	0-00	0.000000
BM106	0.000000	0.000000	0-00	0.000000
BM107	0.000000	0.000000	0-00	0.000000
BNE_T	0.000529	0.000293	173-56	0.000526
BNE_B	0.000934	0.000304	166-28	0.001115
BSW_T	0.000900	0.000534	42-36	0.000645
BSW_B	0.000905	0.000753	31-54	0.001138

Relative Error Ellipses (Meters)
Confidence Region = 95%

Stations From	To	Semi-Major Axis	Semi-Minor Axis	Azimuth of Major Axis	Vertical
BM101	BNE_B	0.000934	0.000304	166-28	0.001115
BM101	BNE_T	0.000529	0.000293	173-56	0.000526
BM102	BNE_B	0.000934	0.000304	166-28	0.001115
BM102	BNE_T	0.000529	0.000293	173-56	0.000526
BM103	BNE_B	0.000934	0.000304	166-28	0.001115
BM103	BNE_T	0.000529	0.000293	173-56	0.000526
BM104	BNE_T	0.000529	0.000293	173-56	0.000526
BM104	BSW_B	0.000905	0.000753	31-54	0.001138
BM104	BSW_T	0.000900	0.000534	42-36	0.000645
BM105	BNE_B	0.000934	0.000304	166-28	0.001115
BM105	BNE_T	0.000529	0.000293	173-56	0.000526
BM105	BSW_B	0.000905	0.000753	31-54	0.001138
BM105	BSW_T	0.000900	0.000534	42-36	0.000645
BM106	BNE_T	0.000529	0.000293	173-56	0.000526

```
BM106      BSW_B          0.000905      0.000753      31-54       0.001138
BM106      BSW_T          0.000900      0.000534      42-36       0.000645
BM107      BNE_T          0.000529      0.000293     173-56       0.000526
BM107      BSW_T          0.000900      0.000534      42-36       0.000645


                          Elapsed Time = 00:00:00

19
42
01 00000001 Top of File
01 00000006 Summary of Files Used and Option Settings
02 00000009 Project Folder and Data Files
02 00000015 Project Option Settings
02 00000033 Instrument Standard Error Settings
03 00000035 Project Default Instrument
01 00000049 Summary of Unadjusted Input Observations
02 00000052 Entered Stations
03 00000054 Fixed Positions
03 00000063 Free Positions
02 00000069 Measured Distance Observations
02 00000091 Zenith Observations
02 00000113 Grid Azimuth/Bearing Observations
01 00000135 Adjusted Bearings and Horizontal Distances
01 00000160 Error Propagation
02 00000163 Station Coordinate Standard Deviations
02 00000178 Station Coordinate Error Ellipses
02 00000195 Relative Error Ellipses
01 00000218 End of File
000030D0
STAR*NET
0000F398
```